

# EXPERIMENTAL AND MODELING STUDY OF URANIUM (6+) SORPTION ON QUARTZ

F. Paul Bertetti, Roberto T. Pabalan, David R. Turner, and Michael Almendarez  
Center for Nuclear Waste Regulatory Analyses, Southwest Research Institute,  
6220 Culebra Road, San Antonio, TX 78238-5166

**Abstract** - Actinides transported in natural environments are typically retarded through sorption processes. Because quartz is a common mineral in rocks and soils, it is important to develop an understanding of the parameters that control actinide sorption on quartz. For instance, geologic units surrounding the proposed high-level nuclear waste repository at Yucca Mountain, Nevada, are composed of up to 30 percent quartz by weight. Experiments were conducted to determine the effects of pH, solid-mass/solution-volume ratio, and uranium concentration in solution on the sorption of uranium(6+) on quartz sand. The experiments were conducted in equilibrium with atmospheric CO<sub>2</sub> in a 0.1 molal NaNO<sub>3</sub> matrix at uranium concentrations of 5, 50 and 500 µg/kg and pH values ranging from 2 to 9. Results indicate that uranium is strongly sorbed on quartz at near-neutral pH. The amount of uranium sorbed is highly dependent on pH and to some extent the total concentration of uranium. Sorption increases as the solid-mass to solution-volume ratio increases. Uranium sorption on quartz is important in the pH range where neutral aqueous uranium species predominate, whereas sorption is inhibited at higher pH where negatively charged carbonate and hydroxy-carbonate-complexes are the predominant uranium species. Relatively simple surface complexation modeling, using a diffuse-layer approach, of the uranium-quartz system adequately reproduces the observed sorption behavior. Effects of sorption competition between quartz and experimental containers are included in the conceptual model.

## INTRODUCTION

A critical concern in the geologic disposal of nuclear wastes is the potential release of radionuclides, particularly actinides such as U, Np, and Pu, to the accessible environment as dissolved constituents in groundwater. Sorption on minerals present along groundwater flow paths may be an important mechanism for attenuating radionuclide migration and release. However, sorption processes are dependent on the properties of both the aqueous phase (e.g., pH, ionic strength, radionuclide concentration, complexing ligands) and the sorptive phase (e.g., composition, surface area, sorption site density, surface charge). Therefore, a quantitative knowledge of actinide sorption behavior and the chemical and physical parameters that affect it is important in evaluating the suitability of proposed geologic repositories for nuclear wastes.

In this study, experiments were conducted to study  $U(6+)$  sorption on quartz, which is a major rock-forming mineral in many geologic environments. In particular, at Yucca Mountain, Nevada, the proposed geologic repository site for U.S. high-level nuclear wastes, quartz makes up nearly one-third of the mass of geologic units surrounding the proposed repository horizon (e.g., Bish and Vaniman, 1985; Bish and Chipera, 1989). By considering quartz separately, the effects of  $U(6+)$  sorption competition from higher affinity minerals can be eliminated, and the conditions in which  $U(6+)$  sorbs onto quartz can be independently evaluated. Uranium was selected as the actinide of interest because it is the predominant heavy metal in spent nuclear fuel (>95%  $UO_2$ ), and its aqueous chemistry is relatively well-understood (e.g., Grenthe et al., 1992). In addition, U solubility in the oxidizing and carbonate-rich groundwaters typical of Yucca Mountain (Kerrisk, 1985) is high, which increases its potential for migration and release to the accessible environment.

The sorption experiments were designed to determine the possible effects of solution pH, solid-mass to solution volume ratio ( $M/V$ ), and solution concentration on  $U(6+)$  sorption onto

quartz. The results were used to develop a thermodynamic model for U(6+) sorption on quartz based on a surface complexation approach in order to permit predictions of U(6+) sorption under other physicochemical conditions. The experiments were conducted over a wide range of solution pH and at several values of M/V and U(6+) concentration to allow comparisons of model predictions with experimental results.

## **EXPERIMENTAL SECTION**

### **PREPARATION OF QUARTZ SUBSTRATE**

Foundry grade quartz sand (Wedron #510), quarried from the St. Peters Sandstone in Illinois, was obtained from Wedron Silica Co., Wedron, Illinois. The sand is comprised almost entirely (>99 percent) of quartz grains. Purity of the sand was checked by x-ray diffraction analysis using a Siemens D-500 diffractometer and Ni-filtered  $\text{CuK}_\alpha$  radiation. The sand's x-ray powder diffraction pattern exhibited no non-quartz peaks. However, petrographic and chemical analyses revealed that some minor impurities were present. When viewed using transmitted and reflected light microscopy, minor mineral impurities (<1 percent), predominantly Fe-oxide grain coatings or pyrite inclusions, were observed. Size separation using U.S. standard sieves indicated that nearly  $94 \pm 1$  percent by weight of the sand was coarser than 0.104 mm and that  $48 \pm 0.5$  percent of the sand consisted of grains between 0.250 mm and 0.149 mm. A larger percentage of the impurities were associated with the finer grain size fractions (<0.074 mm). Chemical analyses by atomic absorption and plasma emission spectrometry confirmed that Al and Fe impurities were present but decreased with increasing grain size. Other investigators have also reported that a significant portion of the non-quartz component of the Wedron sand is associated with the smallest size fractions (Siegel et al., 1993). Based on these analyses and the measured size distribution of Wedron #510 sand, the 0.149–0.250 mm size fraction was selected for use in the sorption experiments.

Because the Fe-oxides and other impurities associated with the quartz could alter results by sorbing U(6+), the selected quartz size fraction was chemically treated to remove soluble salts, carbonates and iron-(hydr)oxides. Soluble salts and carbonates were removed by washing the sand in deionized ultrapure water (~17.8 M $\Omega$ ) and processing it in buffered (pH 5.0) acetic acid solution (Morgan's solution) according to the method of Jackson (1956). Approximately 100 grams of sand were washed in 300 mL of buffer for 30 minutes at 90° C. The solution was then decanted and the process repeated twice more. Following removal of carbonates and soluble salts, the sand was rinsed repeatedly with deionized water, filtered, and dried at 80° C. After drying, the sand was washed in sodium citrate-dithionate-bicarbonate (CDB) solution according to a method modified from Kuntze and Dixon (1986) to remove free iron-(hydr)oxides (e.g., hematite and goethite). About 50 grams of sand were immersed in the CDB solution for 30 minutes at 80° C. The procedure was repeated three times and was followed by rinsing, filtration and drying as done previously. Chemical and petrographic analyses of the treated sand showed a virtual elimination of Fe-oxide coatings on the grains. Minerals and grains (e.g., those with pyrite inclusions) with density above that of quartz (2.65 g/cm<sup>3</sup>) were then removed by density separation using heavy liquid (Na-polytungstate, Geoliquids). Following removal of non-quartz and "heavy" quartz grains, the sand was rinsed and cleaned using an ultrasonic bath and deionized water, then dried at 80°C. Surface area measurement of the 0.149–0.250 mm sand size fraction using N<sub>2</sub>(g) adsorption (BET method) indicated a surface area of 0.03 m<sup>2</sup>/g.

#### URANIUM SOLUTIONS

U(6+) experimental solutions were prepared by dilution of a purchased <sup>233</sup>U standard solution (Isotope Products, Inc.) consisting of 99.5% by mass <sup>233</sup>U. Dilutions were made in a 0.1 molal NaNO<sub>3</sub> matrix. A 500 ppb (μg/kg) U(6+) stock solution was prepared initially, and stock solutions of lower U(6+) concentration (5 and 50 ppb) were prepared by diluting the 500 ppb

U(6+) solution. The stock solutions were sampled immediately before initiation of the experiments to determine the actual initial U(6+) concentration ( $U_{\text{initial}}$ ) of experimental solutions.

Uranium was analyzed by measurement of  $^{233}\text{U}$   $\alpha$ -decay using liquid scintillation counting in a Packard 1900TR or 2505TR/AB liquid scintillation analyzer (LSA). Prior to counting, duplicate 0.5 mL aliquots withdrawn from experimental solutions were acidified with 0.5 mL of 0.02M  $\text{HNO}_3$  solution and then mixed with 5 mL of Ultima-Gold (Packard) scintillation cocktail in a 7-mL glass vial. Acidifying experimental solutions minimizes U(6+) sorption onto the glass LSA vials, which could impact counting results. For the conditions specified, counting efficiency is at or very near to 100 percent for  $\alpha$ -particles, although the energy for the counting region of interest is quenched to 100-350 keV. Because of the purity of the original standard solution and the relatively long half-life of  $^{233}\text{U}$ , the contribution to the total activity of the sample from other alpha- or beta-emitting U isotopes and decay daughters is less than 0.1 percent within the counting region of interest and, therefore, was not considered. Each sample was counted for a period of time such that the  $2\sigma$  error of the reported sample activity in counts per minute (cpm), including background ( $\sim 3$  cpm), was 3% for experimental solutions with initial U(6+) concentrations of 500 or 50 ppb, or 5% for solutions which initially had 5 ppb U(6+). For calculation purposes, raw data in counts per minute, which in this case are equivalent to decays per minute, were converted into concentration units. U(6+) concentrations were subsequently converted into mass (g) of U(6+) using the measured weight of the solution.

## EXPERIMENTAL PROCEDURE

### Sorption Kinetics

Kinetic experiments were conducted to determine the time required to reach sorption equilibrium. These consisted of two mixtures of 50 mL of 50 ppb U(6+) solution and 0.1 g of

quartz sand in 60-mL polycarbonate bottles. Before addition of quartz, the pH of each solution was adjusted from its initial value of ~4.2 to ~5.5 or ~6.5 by addition of NaHCO<sub>3</sub> solution. Measurements of pH were made using a Ross combination electrode and an Orion 920A pH meter. The bottles were kept open to atmosphere and constantly agitated using a gyratory shaker. At specified time intervals, 0.5 mL samples were taken for uranium analysis and the pH of the remaining solutions was measured.

#### Equilibrium Sorption

Equilibrium batch experiments were conducted in 60-mL polycarbonate bottles. The selection of container material is important because different container materials exhibit differing degrees of sorption affinity for U(6+) (Pabalan et al., 1994). Pabalan et al. (1994) showed that under these experimental conditions, polycarbonate containers performed better (i.e., sorbed less U(6+) at a given pH) compared to containers made of Teflon-FEP or polypropylene. Even so, the polycarbonate containers adsorb a significant quantity of U(6+) over the pH range from 4 to 8; thus, the effects of container sorption should be taken into account. Therefore, each experiment was designed to consist of a sorption and a desorption component as described below. This two-phase procedure provided quantitative information on the amounts of U(6+) sorbed onto both the quartz and the containers.

The equilibrium experiments were conducted using initial U(6+) concentrations of 5, 50 or 500 ppb. The U(6+) concentrations used were selected to provide a range of values over which to evaluate U(6+) sorption behavior while keeping the maximum concentration below expected solubility limits for the experimental conditions and the minimum concentration above minimum acceptable values for timely and statistically significant counting of experimental solutions. The solid-mass/solution-volume (M/V) ratio, designed to produce measurable sorption of U(6+) and to minimize variation in M/V due to sample withdrawal and evaporation during the experiments,

was fixed at 2, 20 or 50 g/L. Polycarbonate containers were kept loosely capped to allow equilibrium with atmospheric CO<sub>2</sub>, and the mixtures were agitated using gyratory shakers. Five sets of experiments were conducted, with each set consisting of 29 experimental mixtures at different solution pH. The initial conditions of each experimental set are summarized in Table 1.

The sorption component of each experiment was started by adding approximately 50 g of <sup>233</sup>U solution to each polycarbonate container. The initial pH of each experimental solution was adjusted to a value in the range of 2.0 to 9.0 at approximately 0.25-pH intervals by addition of HNO<sub>3</sub> or NaHCO<sub>3</sub> solution. The amount of reagent needed to achieve the desired initial pH of the U(6+) solutions was estimated using the EQ3NR geochemical code (version 7) with database Data0.com.R12 (Wolery, 1992). For U(6+) solutions with added NaHCO<sub>3</sub>, equilibration with atmospheric CO<sub>2</sub>, as indicated by attainment of constant pH, was reached in about 10 days.

After equilibrium with atmospheric CO<sub>2</sub> was attained, the pH of each solution was measured and solution aliquots were withdrawn to determine the initial mass of U(6+) in solution ( $U_{\text{soln},i}$ ). A weighed amount of quartz was subsequently added to each container. After a sufficient amount of time had elapsed to reach sorption equilibrium, as determined from the kinetics studies, the pH of each solution was remeasured, and solution samples were taken to determine the final mass of U(6+) in solution ( $U_{\text{soln},f}$ ).

The desorption phase of the experiment was subsequently started by quantitatively removing the quartz from each container using Eppendorf micropipets and transferring the quartz (along with some entrained experimental solution) into 50-mL polypropylene test tubes. The contents of each test tube were acidified using small amounts (~3 mL) of 0.1 M HNO<sub>3</sub> to desorb U(6+) from the quartz. After an equilibration period, the mass of U(6+) sorbed on the quartz,  $U_{\text{qtz}}$ , was determined by measuring the amount of U(6+) in the acidified solution in each tube,

$U_{\text{soln,qtzd}}$ , and subtracting the amount,  $U_{\text{soln,transf}}$ , entrained with the aqueous phase during the quartz transfer.

The percent of total U(6+) sorbed onto the quartz,  $\%U_{\text{sorbed,qtz}}$ , was calculated by dividing the mass of U(6+) desorbed from the solid by the total mass of U(6+) available as shown in the following equation:

$$\%U_{\text{sorbed,qtz}} = \frac{U_{\text{soln,qtzd}} - U_{\text{soln,transf}}}{U_{\text{total}} - U_{\text{sample}}} \times 100\% \quad (1)$$

where  $U_{\text{total}}$  is the mass of U(6+) originally added to each experimental container, and  $U_{\text{sample}}$  is the mass of U(6+) calculated to have been removed during sampling for pH and U(6+) concentration during the course of the experiments. The percent of total U(6+) sorbed on the container before addition of the quartz,  $\%U_{\text{cont,i}}$ , was calculated from the equation:

$$\%U_{\text{cont,i}} = \frac{U_{\text{total}} - U_{\text{soln,i}}}{U_{\text{total}}} \times 100\% \quad (2)$$

To determine the percent of total U(6+) sorbed on the containers at the end of the sorption phase of the experiment, the solutions remaining in the polycarbonate containers after withdrawal of the quartz were also acidified using small amounts (~3mL) of 0.1 M HNO<sub>3</sub> and sampled to determine the mass of U(6+) in the acidified solution,  $U_{\text{soln,contd}}$ . The percent U(6+) sorbed on the container after the sorption phase,  $\%U_{\text{cont,f}}$ , was then calculated from:

$$\%U_{\text{cont,f}} = \frac{U_{\text{soln,contd}} - U_{\text{soln,f}} + U_{\text{soln,transf}}}{U_{\text{total}} - U_{\text{sample}}} \times 100\% \quad (3)$$

Calculating  $\%U_{\text{sorbed,qtz}}$  from the amount of U(6+) actually desorbed from the quartz reduces the uncertainty associated with container sorption compared to the typical method of calculating percent sorption from the change in solution concentration. However, the use of Eqn. 1 assumes that the total mass of U(6+) initially added to the experimental containers, corrected for

sampling losses, was available to the quartz. This assumption implies that all the U(6+) sorbed onto the container walls prior to addition of quartz can be desorbed and is available for sorption on the mineral; that is, the effect of sorption on the container is neglected, and the mass of U(6+) sorbed on the container is included as part of  $U_{total}$ .

Mass balance was used to track the total mass of U(6+) in each experiment to confirm reversibility and that desorption was complete. The total mass of U(6+) at the end of the desorption phase of the experiment was compared to the mass of U(6+) at the start of the desorption phase. The percent mass error was calculated from the equation:

$$\% \text{ mass error} = \frac{(U_{\text{soln, qtzd}} + U_{\text{soln, contd}})}{(U_{\text{total}} - U_{\text{sample}})} \times 100\%. \quad (4)$$

Mass balance varied for each experiment primarily due to differences in counting error but averaged better than 2 percent. Mass balance results are included in the summary of experimental data (Table 1).

## EXPERIMENTAL RESULTS

### SORPTION KINETICS

The results of the sorption kinetics experiments are plotted in Fig. 1, which shows the relative amount of uranium lost from each of the two solutions as a function of time. The data indicate that it takes about 200 hr to reach a constant uranium concentration. Based on these data, the equilibrium sorption and desorption mixtures were allowed to react for at least 14 days.

### CONTAINER SORPTION

Figure 2 shows the percent of total U(6+) sorbed on the container as a function of pH before and after addition of quartz in the 50 ppb experiment at  $M/V = 20 \text{ g/L}$ . U(6+) sorption on the polycarbonate containers is significant and shows a strong dependence on solution pH. It reaches a maximum at pH between 6 and 6.5, and decreases towards more acidic or alkaline

conditions. Container sorption decreases, but remains quite significant, after addition of quartz. Data at other experimental conditions (not plotted) indicate that the relative amount of uranium sorbed on the container increases with decreasing initial U(6+) concentration and with decreasing M/V (quartz/solution).

The container sorption data demonstrate that container walls can effectively compete with the mineral substrate for U(6+) and vice versa. This sorption competition between container and mineral surfaces is typically ignored in the sorption literature but contributes uncertainty to published sorption data and to thermodynamic model parameters derived from these data. Our container sorption data show that this sorption competition is a function of pH, U(6+) concentration and M/V. It also depends on the relative sorption affinities of the container and mineral surfaces for the radionuclide of interest; thus, the relative amount of U(6+) sorbed on the container would be much lower in the presence of iron-(hydr)oxides or montmorillonite, which are strong sorbers of uranium. By collecting container sorption data in addition to the data for U(6+) sorption on quartz, it is possible to explicitly account for the effects of container sorption in the conceptual model. Therefore, the effects of container sorption on the total loss of U(6+) from solution were included in the modeling effort (discussed below) by deriving binding constants for U(6+) and polycarbonate containers in addition to binding constants for U(6+) and quartz.

#### QUARTZ SORPTION

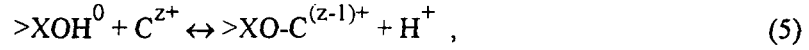
Figures 3(a) and 3(b) show U(6+) sorption on quartz as functions of pH and initial U(6+) concentration ( $U_{\text{initial}}$ ) at M/V ratios equal to 20 and 50 g/L, respectively. The data in these figures demonstrate that U(6+) sorption on quartz is strongly affected by solution pH. U(6+) sorption reaches a maximum at near neutral pH (6.8) and steeply decreases towards acidic or alkaline conditions (sorption and desorption edges, respectively). This dependence of U(6+) sorption on solution pH has also been observed in other studies of U(6+) sorption onto quartz and

other silicate minerals (e.g., Allard et al., 1980; Pabalan et al., 1993; Waite et al., 1994b; Zachara and McKinley, 1994), as well as in studies of U(6+) sorption on aluminum- and iron-(hydr)oxides (e.g., Hsi and Langmuir, 1985; Prikryl et al., 1994; Waite et al., 1994a; Zachara et al., 1987).

Figure 4 compares the results of experiments at an initial U(6+) concentration of 50 ppb and M/V ratios of 2, 20, and 50 g/L. The results show that U(6+) sorption increases with increasing M/V ratio. At lower M/V ratios (2 and 20 g/L), the change in sorption with a change in M/V is approximately linear; e.g., the maximum sorption for the 2 g/L curve is about 4-5%, whereas with a ten-fold increase in M/V (20 g/L) the maximum sorption is approximately 45%. The rise in percent U(6+) sorbed with an increase in M/V apparently results from a corresponding increase in available sorption sites. However, as the M/V ratio continues to increase, the increase in U(6+) sorbed is not proportional (i.e., it exhibits nonlinear behavior). Modeling of data from previous studies shows that as the amount U(6+) sorbed nears 100 percent, sorption becomes insensitive to continued increase in M/V ratio (Turner, 1995)

The initial concentration of U(6+) in solution also influences U(6+) sorption on quartz. As shown in Figure 3, at a fixed M/V, the percent U(6+) sorbed increases as the initial U(6+) concentration decreases. Indeed, when sorption data at a given pH are plotted versus equilibrium concentration in solution, the data fit well a nonlinear Freundlich isotherm (Figure 5). This indicates that sorption of U(6+) on quartz is not proportional to dissolved U(6+) concentration. The trend in adsorption with increasing U(6+) concentration is likely due to the formation of polynuclear aqueous complexes (O'Day, 1994) and is consistent with the postulation that mononuclear U(6+) surface complexes form during U(6+) adsorption (Waite et al., 1994a). The sorption behavior of U(6+) with increasing U(6+) concentration is also indicative of a decrease in the average molar free energy of adsorption with increasing surface coverage (Waite et al., 1994a).

The reasons for the observed dependence on M/V and U(6+) concentration are a consequence of the mass balance and equilibrium chemistry in the U(6+)–quartz system. An equilibrium sorption reaction in the form



where a constant, K, can be defined as the equilibrium constant for the reaction,  $>XOH^0$  represents the concentration of available surface sites, and  $C^{z+}$  and  $>XO-C^{(z-1)+}$  represent a cation in solution and sorbed to the surface, respectively, can be combined with the fraction sorbed (Eq. 1) to give (neglecting activity coefficients, the  $H^+$  term, and sampling losses) an expression that can be used to describe the effects of changing M/V and initial U(6+) concentration on the percent U sorbed by quartz at a given pH:

$$\%U_{\text{sorbed}} \propto \frac{(K) (>XOH^0) (U_{\text{soln},f}) \left(\frac{M}{V}\right)}{U_{\text{initial}}} , \quad (6)$$

As M/V increases, at a given initial U(6+) concentration, the number of available sites also increases, and the relative percent U(6+) sorbed increases. The concentration of U(6+) in solution decreases to compensate for the increase in surface sites. As the initial U(6+) concentration increases, at a given M/V ratio, more surface sites are occupied; the relative percent U(6+) sorbed decreases, and the equilibrium concentration of U(6+) must increase because less surface sites are available.

Although it is convenient to represent adsorption data in terms of percent total U(6+) sorbed, plotting sorption results in terms of a distribution coefficient or K<sub>d</sub> provides a means to normalize the data to sediment concentration (or M/V ratio) and to account for the change (decrease) in aqueous solution concentration during the sorption process. The K<sub>d</sub> may be defined as:

$$K_d \text{ (mL/g)} = \frac{U_{\text{qtz}} / \text{mass quartz (g)}}{U_{\text{soln,f}} / \text{volume solution (mL)}} \quad (7)$$

A plot of log  $K_d$  versus equilibrium pH (Fig. 6) shows the relative effects of changing initial U(6+) concentration. At pH of maximum sorption, the  $K_d$  varies over one order of magnitude for a change in equilibrium U(6+) concentration in solution of two orders of magnitude. The results compare favorably to those of other studies of U(6+) sorption on quartz (Fig. 7). Higher  $K_d$  values reported by Allard et al. (1984), Silva (1992), and Waite et al. (1994b) are likely due to the combined effects of large substrate surface areas and low initial U(6+) concentrations in solution. Normalizing data from Waite et al. (1994b) to the site concentration of quartz used in this study (about a factor of 50 less) results in closer agreement between the two data sets. Reported sorption values for quartz rich tuffs from the Yucca Mountain region are somewhat lower (Thomas, 1987) and are likely indicative of the generally higher initial U(6+) concentrations used in those experiments.

#### **SURFACE COMPLEXATION MODELING**

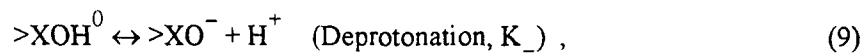
Surface complexation modeling provides a means to interpret chemistry-dependent sorption behavior of actinides in a mechanistic fashion. Different types of surface complexation models (SCMs) have been developed and used to interpret pH-dependent sorption behavior in a number of contaminant-gas-water-solid systems. Among the more commonly used SCM approaches such as the Triple-Layer (TLM), the Constant Capacitance (CCM), and Diffuse-Layer (DLM) models, there is a difference in how the mineral-water interface is represented; all SCM approaches, however, are based on the assumption of analogous behavior between the formation of complexes with functional binding sites at the mineral surface and contaminant complexation by aqueous ligands in the bulk solution (Westall and Hohl, 1980; Davis and Kent, 1990). Through the development of a set of surface reactions, the surface sites are treated effectively as another

ligand competing for the contaminant in SCMs. This allows the development of a geochemical model that can calculate the distribution between sorbed and aqueous phases using mass balance and mass action constraints. For the surface reactions, additional model-dependent terms in the mass action expressions account for the effects of electrostatic interactions at the mineral surface on the system chemistry.

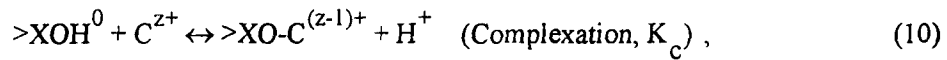
#### DIFFUSE-LAYER MODEL

Typically, SCMs have tended to be applied on a case-by-case basis, with the model parameters adjusted to achieve the best fit to a single data set. This makes it difficult to compare model results in a straightforward manner, since they are frequently based on a different set of reference values. Recent efforts in surface complexation theory have advocated developing a uniform DLM for applications to contaminant sorption (Dzombak and Morel, 1990; Davis and Kent, 1990). Originally developed to model sorption of toxic elements such as Zn, Pb, and Cr on ferrihydrite, the approach of Dzombak and Morel (1990) has also been applied with success to simulate the sorption behavior of actinides such as U and Np (Bradbury and Baeyens, 1993; Turner, 1993, 1995; Pabalan and Turner, 1994; Waite et al., 1994b). The DLM is perhaps the simplest of the SCMs, using a one-layer representation of the mineral-water interface. Although ionic strength effects on the electrostatic interactions are included in the DLM, supporting electrolytes such as  $\text{Na}^+$  and  $\text{NO}_3^-$  are assumed to be inert with respect to the surface, and sorption reactions for these ions are not included explicitly in the geochemical model. Details of the DLM are presented elsewhere (Dzombak and Morel, 1990; Davis and Kent, 1990; Turner, 1993) and only a brief overview will be presented here.

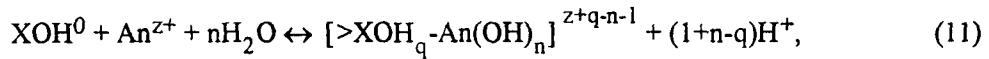
Neutral amphoteric surface sites ( $>\text{XOH}^0$ ) are assumed, through the addition (protonation) or removal (deprotonation) of a proton, to form charged surface sites represented as  $>\text{XOH}_2^+$  and  $>\text{XO}^-$ , respectively. These reactions can be expressed in the form:



where  $K_+$  and  $K_-$  are referred to as the surface acidity constants. The acidity constants  $K_+$  and  $K_-$  are determined by analysis of potentiometric titration data for the mineral of interest (Dzombak and Morel, 1990; Turner, 1993; Turner and Sassman, 1994). The values are specific to a given model and are dependent on the assumptions used, but once they are defined, the acid-base behavior of the surface is characterized, and these values become fixed in the geochemical model. Sorption is represented by postulating the formation of one or more complexes at the mineral-water interface between these sites and the cations and anions in solution. For the DLM, sorption is assumed to take place directly at the mineral surface, forming what are called inner-sphere complexes. For example, a sorption reaction involving the cation  $\text{C}^{z+}$  may be represented as



where the constant  $K_c$  is often referred to as the binding constant and is the remaining adjustable parameter for the DLM. For highly charged species such as the actinides that are readily hydrolyzed [e.g.,  $\text{UO}_2(\text{OH})_n^{2-n}$ ], sorption at the mineral-water interface surface is likely to be complicated by the formation of hydrolyzed surface complexes. A general equation for the formation of mononuclear surface complexes can be written such that:



where  $\text{An}$  represents an actinide with a charge of  $z+$ , and  $q = 0, 1, \text{ or } 2$ , depending on the protonation state of the sorption site. To complete the mass balance for the geochemical model, Dzombak and Morel (1990) calculated the total number of available sites by assuming a constant



specific surface area ( $A_{SP}$ ) and site density ( $N_S$ ) for ferrihydrite. This provides a uniform basis for the model.

Earlier work (Turner, 1993; Turner and Sassman, 1994) has attempted to extend the approach of Dzombak and Morel (1990) to investigate radionuclide sorption on ferrihydrite and other minerals. Although the TLM and CCM were also considered in the earlier work, the current study has adopted a simplified DLM model to maximize the ease of computation and limit the number of required parameters. As recommended by Davis and Kent (1990), the site density of 2.3 sites/nm<sup>2</sup> (Dzombak and Morel, 1990) was assumed for the other minerals and combined with the specific surface area to calculate the total number of available sites. Acidity constants ( $\text{Log } K_+$  and  $\text{Log } K_-$ ) were determined using the non-linear parameter optimization code FITEQL, Version 2.0 (Westall, 1982) to interpret available potentiometric titration data for different minerals (Turner, 1993; Turner and Sassman, 1994). In the absence of data on site heterogeneity for many of the minerals considered, a single-site model was adopted. For minerals with a low zero-point-of-charge ( $\text{pH}_{ZPC}$ ) such as  $\text{SiO}_2$  and  $\text{MnO}_2$ , convergence was difficult to obtain with FITEQL because the titration was typically conducted over a pH range above the  $\text{pH}_{ZPC}$ . In these cases, the formation of only a deprotonated site ( $>XO^-$ ) was assumed (Kent et al., 1988).

FITEQL can also be used to determine the binding constants for the U(6+) sorption reactions. FITEQL requires as input a chemical equilibrium model for the system of interest. This input includes stoichiometries and mass action for aqueous speciation reactions, SCM acidity constants for the protonation and deprotonation of the surface sites [Eqs. (8) and (9)], and assumes a surface complexation reaction of the general form used in Eq. (11). The input file also includes the pH-dependent sorption data to be regressed. Using mass balance and mass-action constraints, FITEQL iteratively adjusts the binding constant for the postulated sorption reaction until the differences between the calculated results and the experimental data are minimized.

Because the binding constant is determined based on the chemical equilibrium model used in the optimization run, the values determined for U(6+) sorption are dependent on the thermodynamic data used in describing the chemical system. If the chemical equilibrium model is modified to include different reactions or updated thermodynamic data, the binding constant may need to be recalculated.

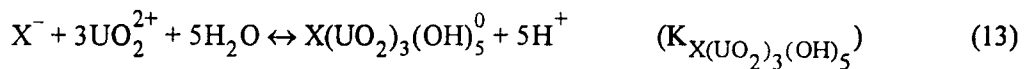
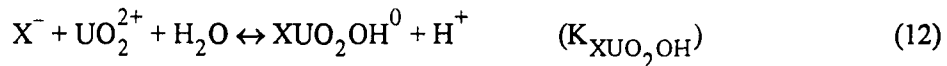
For the purposes of uranium(6+) sorption on quartz, the acidity constant for the  $>\text{SiOH}^0$  site was derived based on interpreting potentiometric titration data for amorphous  $\text{SiO}_2$  as described in Turner (1993). Thermodynamic data for the aqueous speciation in the  $\text{UO}_2\text{-H}_2\text{O-CO}_2$  system were taken from the CNWRA MINTEQA2 database (Turner, 1993), which is based on the NEA Thermodynamic Database for U (Grenthe et al., 1992).

The experimental results presented here for U(6+) sorption on quartz agree with studies for other minerals that have demonstrated a desorption edge develops at high pH in  $\text{UO}_2\text{-H}_2\text{O-CO}_2$  systems (Tripathi, 1984; Hsi and Langmuir, 1985; Pabalan et al., 1993; Prikryl et al., 1994; Waite et al., 1994a). As noted previously (van Geen et al., 1994; Pabalan et al., 1994), one possible explanation for this behavior is the competition for available surface sites by carbonate species such as  $\text{CO}_3^{2-}$  and  $\text{HCO}_3^-$ . Due to a lack of data on carbonate sorption onto quartz, the conceptual model for U(6+) sorption on quartz developed in this study does not explicitly invoke the competition for surface sites by carbonate species (e.g.,  $>\text{SiOH}_2\text{-CO}_3^-$ ). At relatively low carbonate concentrations, this assumption should be reasonable (Zachara et al., 1987). In the conceptual model developed here, the desorption edge at higher pH is assumed to be due to increased aqueous carbonate concentration and the stronger U(6+) affinity for the carbonate ligand relative to the sorption sites, forming aqueous species such as  $\text{UO}_2(\text{CO}_3)_3^{4-}$ . Although this representation may not be entirely accurate, in the absence of definitive data on the

surface complexes being formed (both uranyl and carbonate surface species) it was decided to use the simplest model capable of adequately reproducing the observed sorption behavior.

#### MODELING CONTAINER SORPTION

An additional concern in developing the SCM conceptual model is how to take into account the effects of sorption loss to the container walls. As discussed above, the container effectively competes with the quartz for available U(6+); U(6+) loss to the container is also pH dependent. One approach to incorporating this effect in the chemical model is to develop a set of reactions for sorption onto the container walls. Although the pH dependence suggests that an electrostatic SCM approach might be appropriate, there is no readily available potentiometric titration data from which to extract acidity constants for the container surface. In the absence of these data, we have employed an idealized approach to develop a set of reactions for U(6+) sorption to a hypothetical negatively charged site represented as  $X^-$ . To develop the necessary pH dependence, two reactions binding the positively charged species  $UO_2OH^+$  and  $(UO_2)_3(OH)_5^+$  to the negative  $X^-$  site were considered:



In the pH range of interest (4 to 8), both  $UO_2OH^+$  and  $(UO_2)_3(OH)_5^+$  are common aqueous species, and the single positive charge makes the reactions electrostatically favorable. Once binding constants are determined for these reactions, they can be included in the chemical equilibrium model for the overall sorption. In this manner, competition between the container and the mineral can be accounted for in developing the DLM parameters. It may be possible to use a

similar approach to progressively build in complexity into sorption models involving competition in multi-mineral systems.

The data for loss to the container prior to the addition of quartz to the  $\text{UO}_2\text{-H}_2\text{O-CO}_2$  system was interpreted using FITEQL to determine binding constants for the reactions given in Eqs. (12) and (13). The remaining condition to be determined is the total concentration of the hypothetical site  $X^-$  ( $T_{X^-}$ ). Without independent data on site density, it was decided to use FITEQL to simultaneously determine  $K_{X\text{UO}_2\text{OH}}$ ,  $K_{X(\text{UO}_2)_3(\text{OH})_5}$ , and  $T_{X^-}$ . The resulting values are given in Table 2, and the DLM results are shown in Figure 8. The site density given for the container in Table 2 is based on a measured area of  $64.8 \text{ cm}^2$  ( $6.48 \times 10^{15} \text{ nm}^2$ ) of container surface in contact with the solution.

Despite the large number of assumptions made, the model shows promise for using this type of approach to reproduce the observed container sorption. There is room for improvement, however, ideally through a more careful characterization of the polycarbonate surface. Unlike an SCM approach, the current container sorption model does not take into account electrostatic effects at the polycarbonate-solution interface. It is not clear if potentiometric titration is possible on the flask itself, allowing the development of SCM acidity constants for the container walls. Also, differences in container losses under similar experimental conditions suggest that there are inconsistencies between different batches of polycarbonate that may make it difficult to develop a single set of parameters for the container surface (Pabalan et al., 1994). The lack of surface consistency might be due to processes such as differences in manufacturing conditions or feedstock materials, bottle preparation, or surface abrasion, effects which are difficult to characterize for the purposes of modeling.

## MODELING QUARTZ SORPTION

With parameters in place for the container surface, FITEQL was used to determine the DLM parameters for U(6+) sorption on quartz. The binding constants for the reactions in Eqs. (12) and (13) were included in the chemical equilibrium model to account for competition between the container and the quartz. Using the data from the experiment at initial U(6+) concentration of 50 ppb and M/V=20 g/L, FITEQL-derived binding constants (Table 2) were used in the geochemical speciation code MINTEQA2 (Allison et al., 1991) to reproduce U(6+) sorption behavior onto quartz and polycarbonate for all experimental conditions (Fig. 9). Equilibrium constants in the MINTEQA2 database for aqueous speciation reactions in the  $\text{UO}_2\text{-H}_2\text{O-CO}_2$  system are the same as those used in the FITEQL chemical equilibrium model. Given the complex aqueous speciation in the  $\text{UO}_2\text{-H}_2\text{O-CO}_2$  system, it is perhaps not surprising that several reactions were necessary to reproduce the observed sorption behavior.

Review of the sorption model curves reveals that the model is able to predict the general trends in the effects of changing M/V and U(6+) concentration. The model generally reproduced the sorption and desorption edges reasonably well at lower M/V and higher U(6+) concentration, but underpredicted the maximum sorption for higher M/V and lower U(6+) concentration. If the binding constants are increased to match the sorption maximum, then the model sorption envelope is typically too broad for the observed data. It is possible that different surface complexes form at lower site coverages (higher M/V and/or lower U(6+) concentration). This is supported by the differences in uranium speciation at 5, 50, and 500 ppb (Turner, 1993). It is also possible that site heterogeneities may require a two-site model like that proposed for ferrihydrite by Dzombak and Morel (1990). Adoption of a two-site model, however, would also require development of a second set of binding constants. Additionally, the model developed for loss to the container walls is idealized. More careful characterization of the polycarbonate surface may

allow refinement of models of the container surface, leading to a better representation of the competition between the container walls and the sorbing mineral.

The DLM results for U(6+) sorption on quartz and polycarbonate can be deconvoluted to show the predicted sorption on just the quartz. Unfortunately, the predicted curve for sorption onto quartz does not match the experimental data as well as the predicted curves for the total sorption data (Fig. 10). Although the trends of increasing sorption with increasing M/V are correct, the sorption envelope is too broad and underpredicts the maximum sorption observed. The DLM results can be improved by considering only the quartz data in the FITEQL optimization and by postulating a different surface reaction using one of two neutral species predicted to be present in solution over the pH range from 5 to 8,  $\text{UO}_2\text{CO}_3^0$  (Fig 10, Table 2). The sorption of U(6+) is better represented, but lost is the ability to account for the other sorptive phase, in this case the polycarbonate container. This dilemma points out the difficulties in trying to model more complex systems while maintaining a simplified modeling approach.

Finally, the calculated distribution, for the case including both quartz and container sorption, of uranyl species on surfaces and in solution for a U(6+) concentration of 50 ppb and an M/V=20 g/L (Fig. 11) shows that sorption over the pH range from 4 to 8 is dominated by neutral and univalent positively charged U(6+) species. Slight differences in published log K values versus the actual log K values for these species could result in the fit errors observed. Similarly, model overestimation of the influence of carbon species (e.g.,  $\text{UO}_2(\text{CO}_3)_2^{2-}$ ) could result in the underestimation of sorption near pH 7. Another aspect to consider is that the modeling approach does not allow for automatic iterative regression of all possible species at once. As such, the analogous aqueous species reactions may be inadequate or the proper combination of species may not have been selected.

The current efforts to develop surface complexation models that can account for some of the competing sorption processes show promise in describing and predicting U(6+) sorption on quartz as well as actinide sorption on other minerals. Developing approaches that are based on geochemical principles, such as the DLM, allows quantitative examination of sorption under physicochemical conditions outside experimental values in a way that is beyond the capabilities of purely empirical approaches. Constructing the conceptual model of the mineral-water interface using a set of reactions of the form given in Eqs. (8) through (10) allows the application of mass balance and mass action constraints to determine sorption as a function of system chemistry. For example, since  $H^+$  is the potential determining ion, the protonation/deprotonation of the surface sites and the formation of surface complexes can be written in the form of reactions that are functions of pH; the ability to incorporate these reactions in a chemical equilibrium model of the system of interest enables a mechanistic approach such as the DLM to simulate the pH-dependent sorption behavior observed for the actinides. Similarly, the model can also be adapted to predict the effects of changes in M/V ratio and total carbon.

### CONCLUSIONS

Quartz, a common component of the rock matrix in units surrounding the proposed high-level nuclear waste repository at Yucca Mountain, Nevada, adsorbs U(6+) in the pH range (~6.5 to 8) typical for Yucca Mountain groundwaters. When surface area and U(6+) concentration effects are taken into account, the observed magnitude of U(6+) sorption onto quartz adequately corresponds to that observed in previous studies. Because the relative sorption affinity of quartz for U(6+) is low, sorption of U(6+) onto the experimental containers was significant and was accounted for both in the experimental design and the modeling of U(6+) sorption behavior.

Batch type experiments can provide valuable information regarding basic sorption behavior and the ability to model that behavior. While experiments that include mixed substrates

and more complex solution chemistries (e.g., multiple actinides) are important, it can be difficult to resolve sorption behavior in multiple mineral systems without prior knowledge of the sorption behavior of the individual minerals present. Additionally, batch experiments on mineral separates provide a means to identify similarities in the sorption behavior of a particular actinide.

The experimental data reported here and in previous studies (e.g., Hsi and Langmuir, 1985; Pabalan and Turner, 1994; Waite et al., 1994a; 1994b; Turner, 1995) demonstrate that U(6+) sorption on quartz, montmorillonite, clinoptilolite,  $\alpha$ -alumina, and Fe-oxides, which are sorbents of distinct mineralogic and surface properties, is strong at near-neutral pH (~6.3 to 6.8). In all those cases, the amount of U(6+) sorbed is strongly dependent on pH and decreases steeply away from near-neutral pH. The M/V ratio (or analogously, surface-area to solution-volume ratio) also influences sorption; that is, as the ratio increases, the amount of U(6+) sorbed on the solid also increases. The similarities in sorption characteristics of these minerals imply that solution chemistry and substrate site density may be the most important parameters needed to describe U(6+) sorption and that specific mineralogic sorption data is secondary. Because of the strong dependence on pH and M/V ratio, modeling sorption processes will likely require that changes in groundwater chemistry and in rock/fluid ratio be properly accounted for in performance assessment calculations if retardation by sorption processes is included.

Given the complexity of actinide chemistry, it is likely that surface complexation models represent a simplification of the mineral-water interface. Although the models define one or more surface reactions, there is typically a lack of independent analytical data supporting the formation of a particular surface complex. In the absence of these data, the exact form of the surface reaction is generally selected by the modeler based on the analogous reactions in aqueous speciation. While the ability of the model to reproduce the observed trends in sorption behavior shows the promise of a uniform SCM approach, even in a complicated system like UO<sub>2</sub>-H<sub>2</sub>O-CO<sub>2</sub>, the

resultant degradation in model performance and increase in model complexity associated with attempts to describe the system in detail highlight the need for further work before SCMs can directly contribute to the regulatory or decision making process regarding disposal of high-level nuclear wastes.

#### Acknowledgments

Reviews by B. Murphy and D. Pickett significantly improved an early draft of this paper. This work was funded by the U.S. Nuclear Regulatory Commission (NRC), Office of Nuclear Regulatory Research, Division of Regulatory Applications (G. Birchard, project officer) under Contract No. NRC-02-93-005. This paper is an independent product of the CNWRA and does not necessarily reflect the views or the regulatory position of the NRC. Use of commercial product and manufacturer names is for accuracy in technical reporting only and does not imply endorsement by the CNWRA or the NRC.

#### REFERENCES

- Allard B., Beall G. W. and Krajewski T. (1980) The sorption of actinides in igneous rocks. *Nuclear Technol.* **49**, 474–480.
- Allard B., Olofsson U. and Torstenfelt B. (1984) Environmental actinide chemistry. *Inorganica Chimica Acta* **94**, 205–224.
- Allison J. D., Brown D. S. and Novo-Gradac K. J. (1991) *MINTEQA2/PRODEFA2, A Geochemical Assessment Model for Environmental Systems: Version 3.0 User's Manual*. EPA/600/3-91/021 Environmental Research Laboratory, Office of Research and Development, U.S. Environmental Protection Agency, Athens, GA.
- Bish D. L. and Chipera S. J. (1989) *Revised Mineralogic Summary of Yucca Mountain, Nevada*. Report LA-11497-MS, Los Alamos National Laboratory, Los Alamos, NM.

- Bish D. L. and Vaniman D. T. (1985) *Mineralogic Summary of Yucca Mountain, Nevada*. LA-10542-MS, Los Alamos National Laboratory, Los Alamos, NM.
- Bradbury M. H. and Baeyens B. (1993) A general application of surface complexation to modeling radionuclide sorption in natural systems. *J. Colloid Interface Sci.* **158**, 364–371.
- Davis J. A. and Kent D. B. (1990) Surface complexation modeling in aqueous geochemistry. In *Reviews in Mineralogy: Mineral-Water Interface Geochemistry* (eds M.F. Hochella, Jr. and A.F. White) Vol. 23., pp. 177–260. Mineralogical Society of America, Washington, DC.
- Dzombak D. A. and Morel F. M. M. (1990) *Surface Complexation Modeling: Hydrous Ferric Oxide*. John Wiley and Sons, New York, NY.
- Grenthe I., Fuger J., Konings R., Lemire R., Muller A., Nguyen-Trung C. and Wanner H. (1992) *Chemical Thermodynamics of Uranium*. North-Holland, Amsterdam.
- Hsi C. D. and Langmuir D. (1985) Adsorption of uranyl onto ferric oxyhydroxides: Application of the surface complexation site-binding model. *Geochim. Cosmochim. Acta* **49**, 1931–1941.
- Jackson M. L. (1956) *Soil Chemical Analyses - Advanced Course*. (Fourth Printing, 1968) Published by the Author, Department of Soil Science, University of Wisconsin, Madison.
- Kent D. B., Tripathi V. S., Ball N. B., Leckie, J. O. and Siegel M. D. (1988) *Surface-Complexation Modeling of Radionuclide Adsorption in Subsurface Environments*. NUREG/CR-4807. Nuclear Regulatory Commission, Washington, D.C.
- Kerrisk J. F. (1985) *An Assessment of the Important Radionuclides in Nuclear Waste*. LA-10414-MS, Los Alamos National Laboratory, Los Alamos, NM.
- Kuntze G. W. and Dixon J. B. (1986) Pretreatment for mineralogical analysis. In *Methods of Soil Analysis, Part I. Physical and Mineralogical Methods. Agronomy Monograph no. 9* (2nd edition) (ed A. Klute), pp. 91–100. American Society of Agronomy and Soil Science Society of America, Madison, WI.

O'Day P. A. (1994) Free energies of adsorption of divalent metal ions on quartz. *GSA Abstracts with Programs* 26(7), 1994 Annual Meeting, p. A-111. Geological Society of America, Boulder, CO.

Pabalan R. T., Prikryl J. D., Mueller P. M. and Dietrich T. B. (1993) Experimental study of U(6+) sorption on the zeolite mineral clinoptilolite. In *Scientific Basis for Nuclear Waste Management XVI - MRS Symposium Proceedings* (eds C. G. Interrante and R. T. Pabalan), Vol. 294, pp. 777-782, Materials Research Society, Pittsburgh, PA.

Pabalan R. T. and Turner D. R. (1994) Sorption Modeling for HLW Performance Assessment. *NRC High-Level Radioactive Waste Research at CNWRA July-December, 1993* (ed B. Sagar), CNWRA 93-02S, pp. 8-1 to 8-23. Center for Nuclear Waste Regulatory Analyses, San Antonio, TX.

Pabalan R. T., Turner D. R. and Bertetti F. P. (1994) Sorption Modeling for HLW Performance Assessment. *NRC High-Level Radioactive Waste Research at CNWRA January-June, 1994* (ed B. Sagar), CNWRA 94-01S, pp. 77-95. Center for Nuclear Waste Regulatory Analyses, San Antonio

Prikryl J. D., Pabalan R. T., Turner D. R. and Leslie B. W. (1994) Uranium Sorption on  $\alpha$ -alumina: Effects of pH and surface-area/solution-volume ratio. *Radiochim. Acta* **66/67**, 291-296.

Siegel M. D., Ward D. B., Cheng W. C., Bryant C., Chaocas C. S. and Reynolds C. G. (1993) Preliminary characterization of materials for a reactive transport model validation experiment. In *High-Level Radioactive Waste Management, Proceedings of the Fourth International Conference*, pp. 348-356. American Nuclear Society and American Society of Civil Engineers, La Grange Park, IL.

- Thomas K. W. (1987) *Summary of Sorption Measurements Performed with Yucca Mountain, Nevada, Tuff Samples and Water from Well J-13*. LA-10960-MS, Los Alamos National Laboratory, Los Alamos, NM.
- Tripathi V. S. (1984) *U(VI) Transport Modeling: Geochemical Data and Submodels*. Ph.D. Dissertation. Stanford University, Stanford, CA.
- Turner D. R. (1993) *Mechanistic Approaches to Radionuclide Sorption Modeling*. CNWRA 93-019, Center for Nuclear Waste Regulatory Analyses, San Antonio, TX.
- Turner D. R. (1995) *A Uniform Approach to Surface Complexation Modeling of Radionuclide Sorption*. CNWRA 95-001, Center for Nuclear Waste Regulatory Analyses, San Antonio, TX.
- Turner D. R. and Sassman S. A. (1994) Approaches to sorption modeling for high-level waste performance assessment. *Radiochim. Acta* **66/67**, 745–756.
- van Geen A., Robertson A. P. and Leckie J. O. (1994) Complexation of carbonate species at the goethite surface: Implications for adsorption of metal ions in natural waters. *Geochim. Cosmochim. Acta* **58**, 2,073–2,086.
- Waite T. D., Davis J. A., Payne T. E., Waychunas G. A. and Xu N. (1994a) Uranium(VI) adsorption to ferrihydrite: Application of a surface complexation model. *Geochim. Cosmochim. Acta* **58**, 5465–5478.
- Waite T. D., Payne T. E., Davis J. A. and Sekine K. (1994b) Uranium Sorption Modeling - A Surface Complexation Approach. In *Nuclear Science and Technology, Fifth CEC Natural Analogue Working Group Meeting and Alligator Rivers Project (ARAP) Final Workshop Proceedings* (eds H. von Maravic and J. Smellie). EIR-15176, p. 95–100.
- Westall J. C. (1982) FITEQL: *A Computer Program for Determination of Chemical Equilibrium Constants from Experimental Data, Version 2.0*. Report 82-02, Oregon State University, Department of Chemistry, Corvallis, OR.

Westall J. C. and Hohl H. (1980) A comparison of electrostatic models for the oxide/solution interface. *Advances in Colloid and Interface Science* **12**, 265-294.

Wolery T. J. (1992) *EQ3/6, A software package for geochemical modeling of aqueous systems: Package overview and installation guide (version 7.0)*. UCRL-MA-110662 PT 1, Lawrence Livermore National Laboratory, Livermore, CA.

Zachara J. M., Girvin D. C., Schmidt R. L. and Resch C. T. (1987) Chromate adsorption on amorphous iron oxyhydroxide in the presence of major groundwater ions. *Environ. Sci. Technol.* **21**, 589–594.

Zachara J. M. and McKinley J. P. (1994) Influence of hydrolysis on the sorption of metal cations by smectites: Importance of edge coordination reactions. *Aquatic Sci.* **55**, 250–261.

## FIGURE CAPTIONS:

Figure 1: Results of kinetics experiments. Initial U(6+) concentration is 50 ppb and M/V ratio is 2 g/L. Circles and squares represent data for mixtures with initial pH of 6.1 and 5.4, respectively. Best fit curves are added as aids to the eye only.

Figure 2: U(6+) sorption on polycarbonate container as a function of pH. Container sorption before ( $\%U_{\text{cont},i}$ ) and after ( $\%U_{\text{cont},f}$ ) addition of quartz are represented by filled and unfilled circles, respectively. Data are from experiments with initial U(6+) concentration of 50 ppb and M/V of 20 g/L. Error bars represent calculated total uncertainties based on  $1\sigma$  error.

Figure 3: Sorption of U(6+) on quartz as a function of initial U concentration and pH: (a) U(6+) sorption data for experiments at initial U(6+) concentrations of 5 and 50 ppb and an M/V ratio of 20 g/L; (b) U(6+) sorption data at initial U(6+) concentrations of 50 and 500 ppb and an M/V ratio of 50 g/L.

Figure 4: Sorption of U(6+) on quartz as a function of M/V ratio and pH. The experiments were conducted at an initial U(6+) concentration of 50 ppb and at M/V ratios of 2, 20, or 50 g/L.

Figure 5: Freundlich isotherms of U(6+) sorption data at pH 6, 6.5, and 7. Data are fitted by nonlinear least squares regression using the equation  $S=KC^n$ , where S is the concentration of U(6+) on the quartz, C is the concentration of U(6+) in solution, and K and n are constants. Values of n below 1 indicate a nonlinear trend in the increase of sorbed concentration with increased solution equilibrium concentration of U(6+).

Figure 6: Log  $K_d$  (g/mL) of quartz sorption data as a function of equilibrium pH.

Figure 7: Comparison of data for U(6+) sorption on quartz. All data collected under atmospheric conditions and converted to  $K_d$  (g/mL). Data from this study are labeled with associated initial solution U(6+) concentration and M/V ratio. Data from Waite et al. (1994b) were determined at  $[U(6+)] = 1 \times 10^{-6} M$  (~238 ppb) and  $M/V = 100$  g/L using a size fraction between 0.008 and 0.015 mm (equivalent surface area ~50 times that used in this study). Data from Silva (1992) collected using Min-U-Sil quartz and  $[U(6+)] = 1 \times 10^{-6} M$ . Data from Allard et al. (1984) were collected using natural quartz and  $[U(6+)] = 1 - 5 \times 10^{-11} M$  (~0.005 ppb) (surface area not available). Data from Thomas (1987) represent sorption experiments on devitrified tuff core samples with predominant quartz and feldspar mineralogy (cores: G1-1982, G1-2333, YM-22, and JA-32) with  $[U(6+)] = 2 \times 10^{-7} - 5 \times 10^{-6} M$  (~50-1000 ppb). Error bars give range of reported  $K_d$  values. Curves are added as aids to the eye only.

Figure 8: Results for model of U(6+) sorption onto polycarbonate as a function of pH. Data represents the average sorption of U(6+) onto containers before addition of quartz in experiments with  $[U(6+)] = 50$  ppb.

Figure 9: Diffuse-Layer Model results for U(6+) sorption onto quartz and polycarbonate as a function of pH. FITEQL-derived binding constants determined using data at initial  $[U(6+)] = 50$  ppb and  $M/V = 20$  g/L. (a) Model predictions at  $M/V = 50$  g/L for  $[U(6+)] = 500$  ppb and 50 ppb. (b) Model predictions for varying  $M/V$  at initial  $[U(6+)] = 50$  ppb.

Figure 10: Comparison of DLM results for U(6+) sorption onto quartz as determined by (i) deconvolution of the quartz sorption component of the total sorption model (solid curve) or (ii) independent fit of quartz sorption data using a single surface reaction (dashed curve).

Figure 11: MINTEQA2 calculated distribution of uranyl species in solution (open symbols) and on the quartz and polycarbonate surface (closed symbols) at [U(6+)]=50 ppb and M/V=20 g/L. To improve clarity of the figure, aqueous species contributing to less than 5 percent of the total distribution over the pH range of 2–9 and the sorbed species  $>\text{SIO-UO}_2(\text{OH})_2^{2-}$  are not plotted.

**Table 1. Summary of experiments**

Experiment	[U] (ppb)	M/V (g/L)	Mass Quartz (g)	Average Mass Balance Error	2 $\sigma$ Counting Error
Q1	50	2	0.1	-1.42 $\pm$ 1.5%	3%
Q2	50	20	1.0	-0.49 $\pm$ 1.0%	3%
Q3	50	50	2.5	0.20 $\pm$ 1.3%	3%
Q4	5	20	1.0	-1.26 $\pm$ 1.9%	5%
Q5	500	50	2.5	-0.51 $\pm$ 1.6%	3%

**Table 2. Summary of DLM parameters**

Surface Reactions	log K	Notes
$>\text{SiOH}^0 \leftrightarrow >\text{SiO}^- + \text{H}^+$	-7.2	a
$\text{X}^- + \text{UO}_2^{2+} + \text{H}_2\text{O} \leftrightarrow \text{XUO}_2\text{OH}^0 + \text{H}^+$	2.7	b, c
$\text{X}^- + 3\text{UO}_2^{2+} + 5\text{H}_2\text{O} \leftrightarrow \text{X}(\text{UO}_2)_3(\text{OH})_5^0 + 5\text{H}^+$	-3.2	b, c
$>\text{SiOH}^0 + \text{UO}_2^{2+} \leftrightarrow >\text{SiO-UO}_2^+ + \text{H}^+$	0.8	d, e
$>\text{SiOH}^0 + \text{UO}_2^{2+} + \text{H}_2\text{O} \leftrightarrow >\text{SiO-UO}_2\text{OH}^0 + 2\text{H}^+$	-5.4	d, e
$>\text{SiOH}^0 + \text{UO}_2^{2+} + 2\text{H}_2\text{O} \leftrightarrow >\text{SiO-UO}_2(\text{OH})_2^- + 3\text{H}^+$	-12.6	d, e
$>\text{SiOH}^0 + \text{UO}_2^{2+} + \text{CO}_3^{2-} \leftrightarrow >\text{SiOH-UO}_2\text{CO}_3^0$	16.4	f
<p>(a) From Turner (1993)            (b) Site Density (<math>\text{Tx}^-</math>, Container) = 0.1 sites/nm<sup>2</sup> (Determined using FITEQL)            (c) From FITEQL fit of average container sorption without quartz [U(6+)] initial = 50 ppb            (d) Site Density (Quartz) = 2.3 sites/nm<sup>2</sup> (from Dzombak and Morel, 1990); Quartz Specific Surface Area (<math>A_{\text{Sp}}</math>) = 0.03 m<sup>2</sup>/g            (e) From FITEQL fit of total sorption (quartz and polycarbonate) data [U(6+)] initial = 50 ppb and M/V = 20 g/L            (f) From FITEQL fit of quartz sorption data (pH 4-8) [U(6+)] initial = 50 ppb and M/V = 20 g/L</p>		

Figure 1

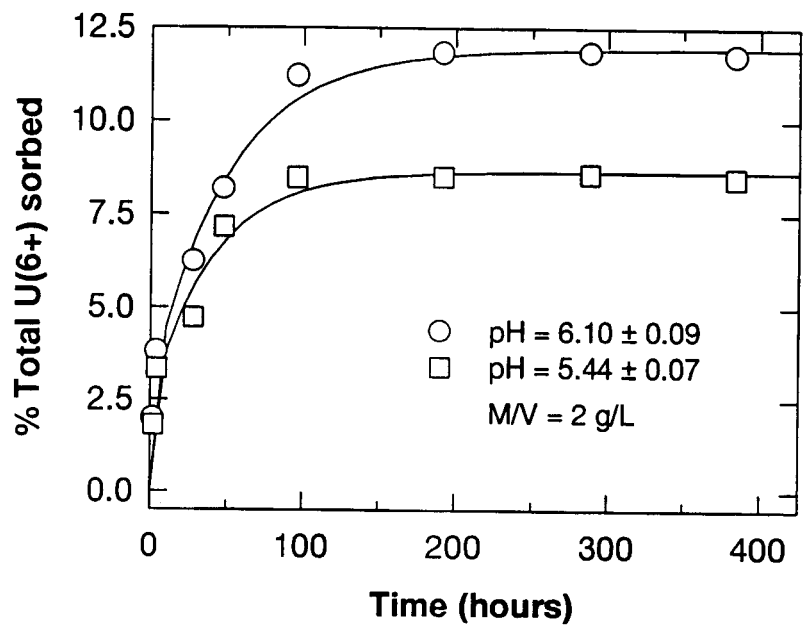


Figure 2

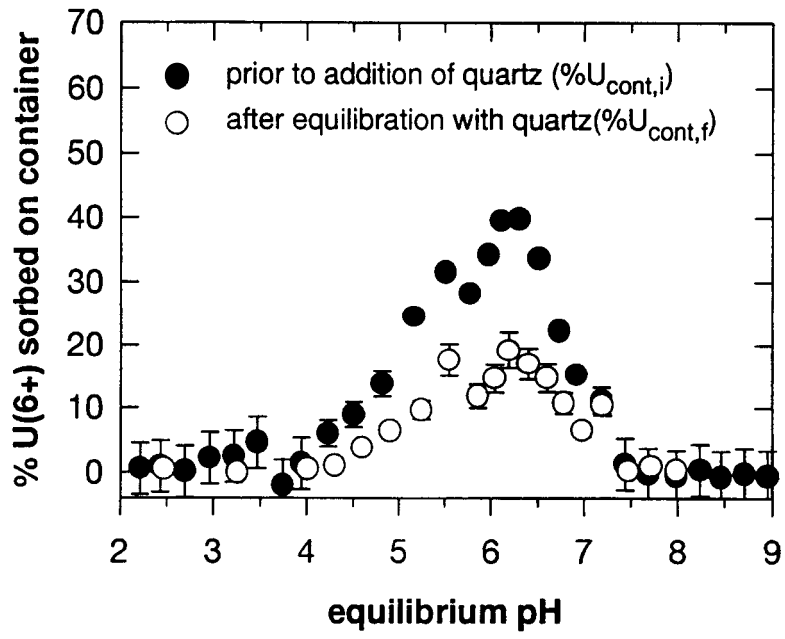


Figure 3(a)

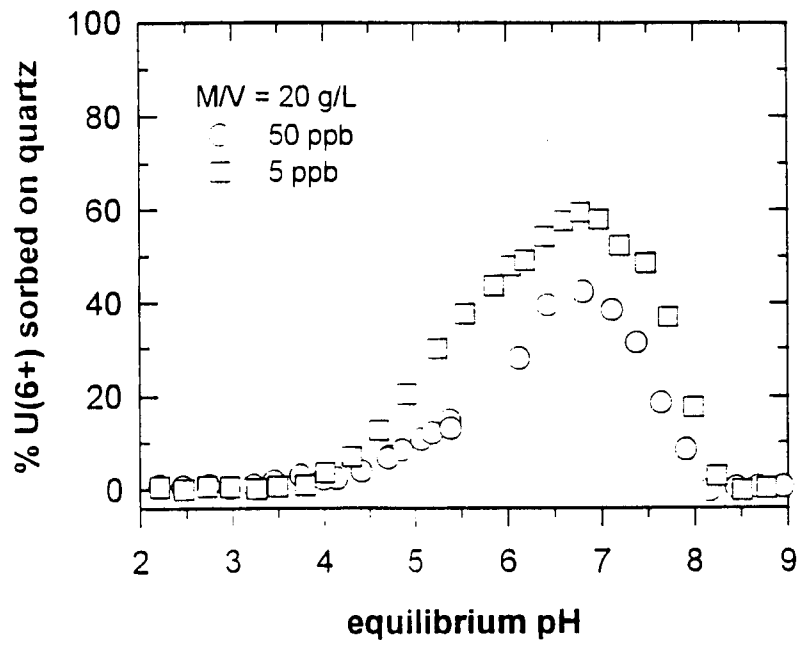


Figure 3(b)

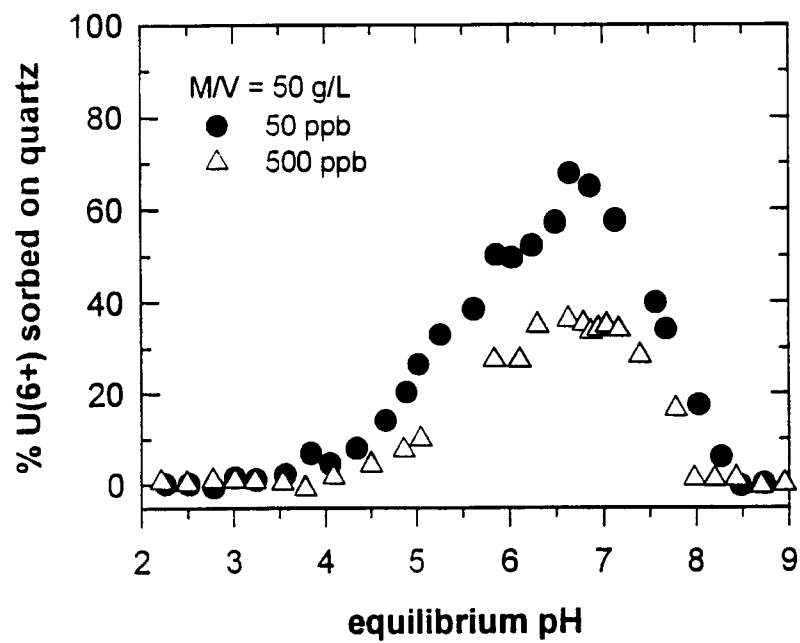


Figure 4

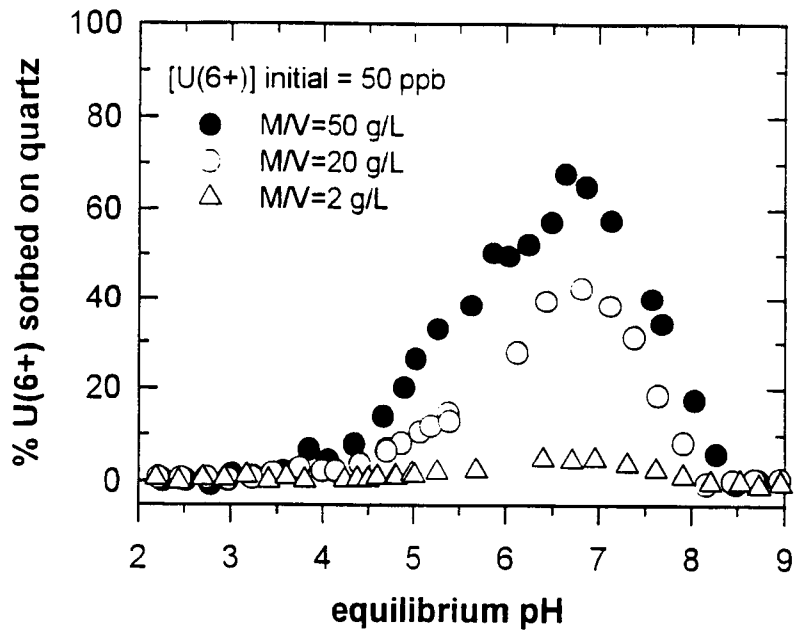


Figure 5

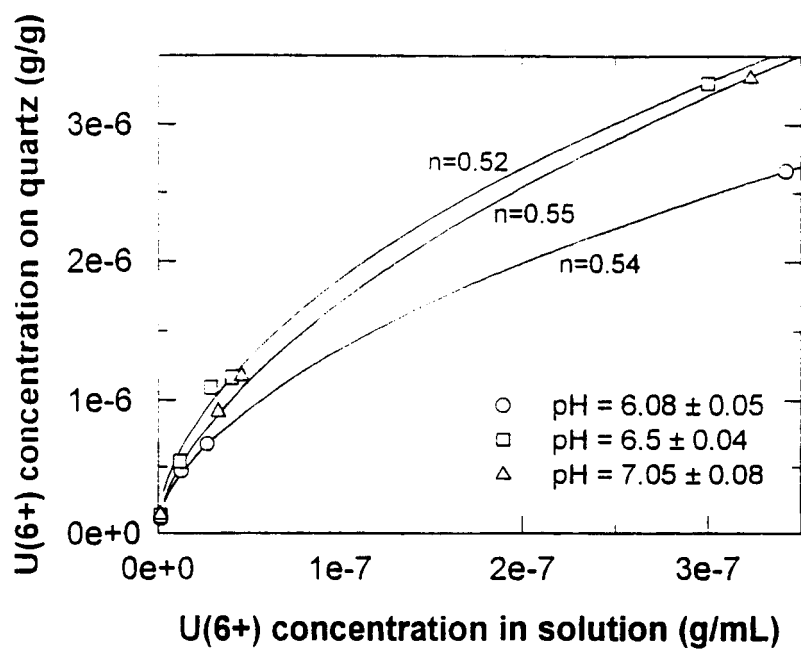


Figure 6

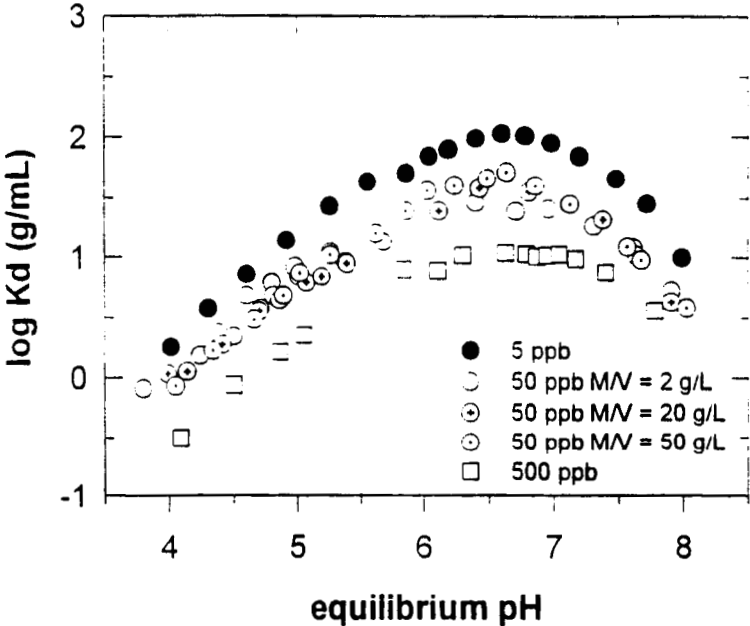


Figure 7

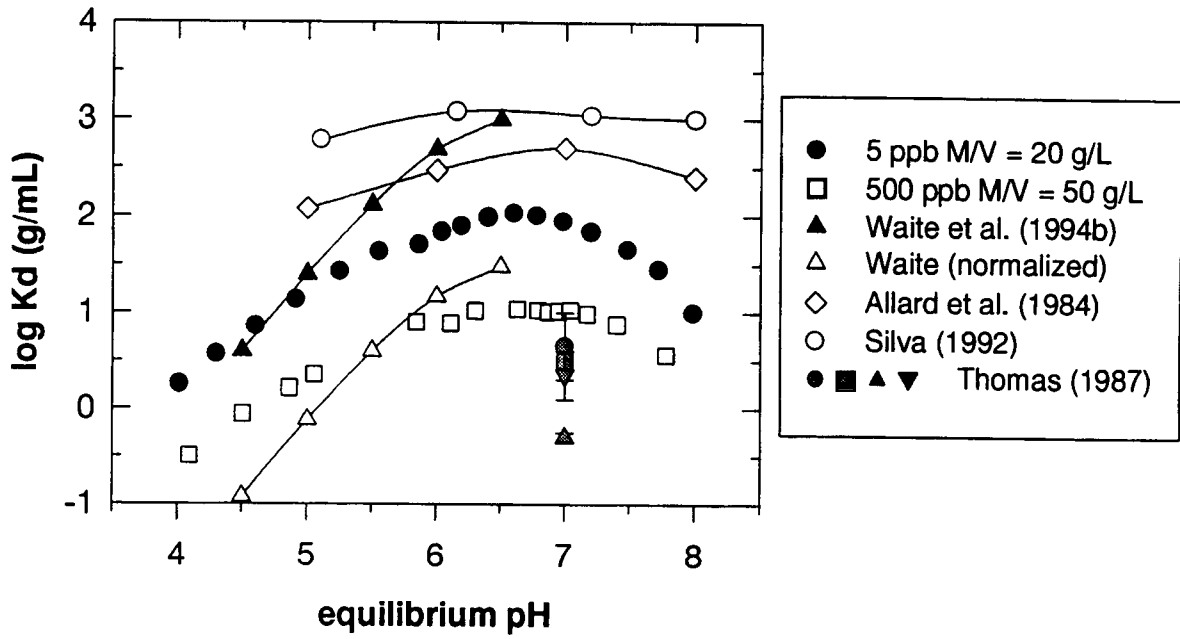


Figure 8

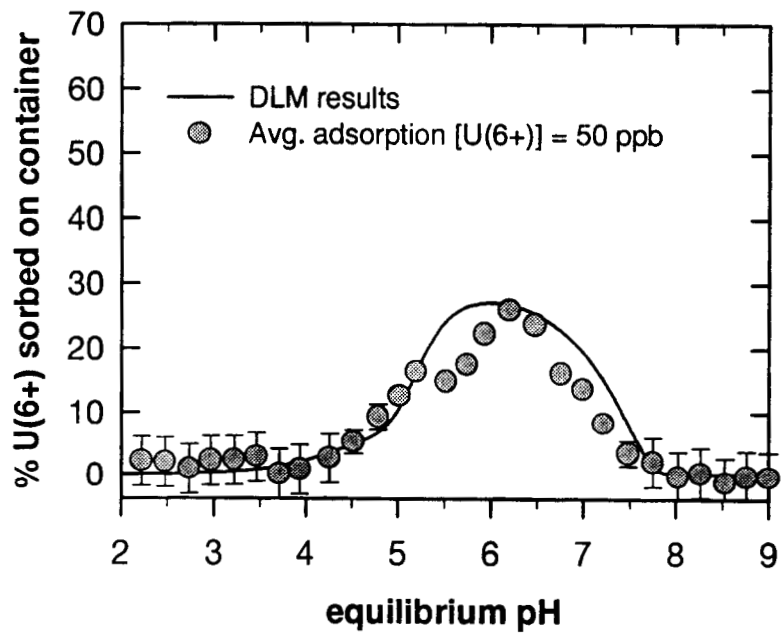


Figure 9(a)

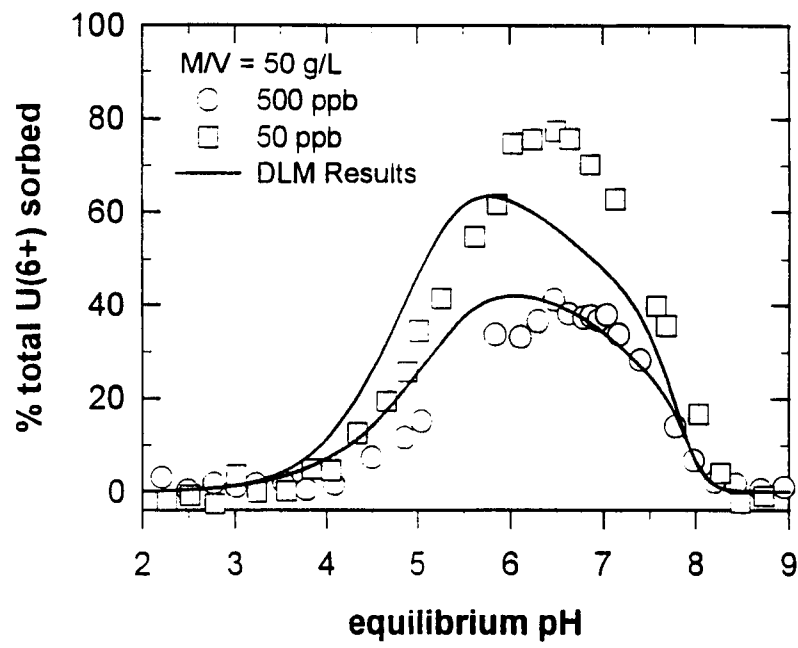


Figure 9(b)

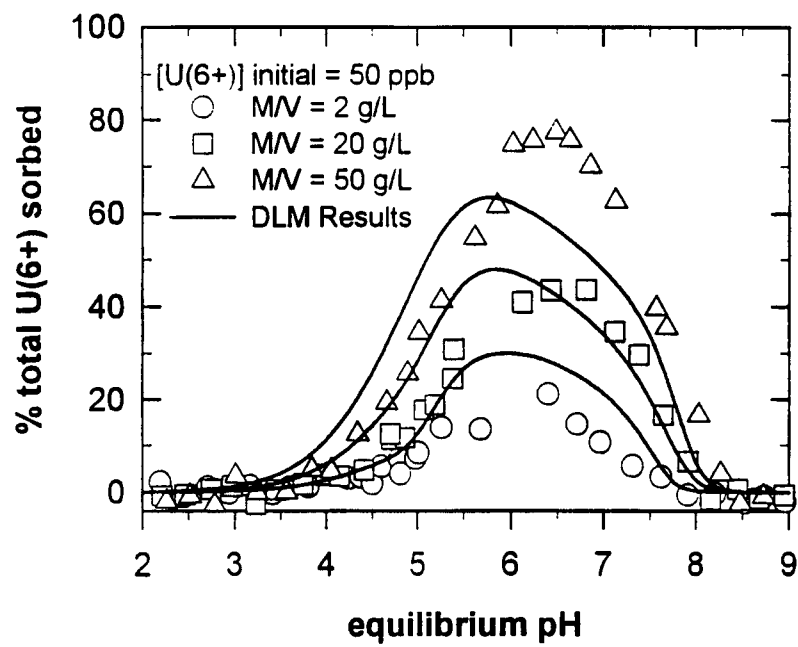


Figure 10

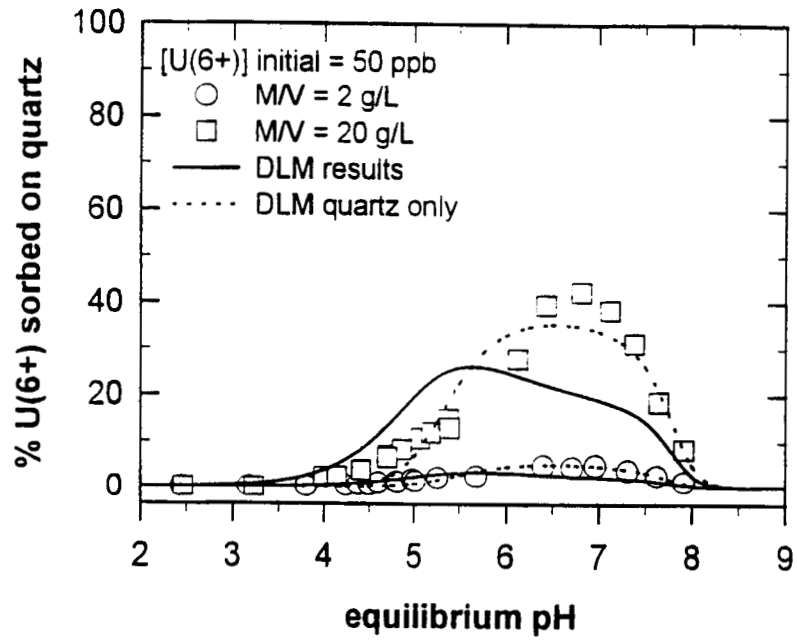


Figure 11

